

Journal of Materials Chemistry B

Accepted Manuscript



This is an *Accepted Manuscript*, which has been through the Royal Society of Chemistry peer review process and has been accepted for publication.

Accepted Manuscripts are published online shortly after acceptance, before technical editing, formatting and proof reading. Using this free service, authors can make their results available to the community, in citable form, before we publish the edited article. We will replace this *Accepted Manuscript* with the edited and formatted *Advance Article* as soon as it is available.

You can find more information about *Accepted Manuscripts* in the [Information for Authors](#).

Please note that technical editing may introduce minor changes to the text and/or graphics, which may alter content. The journal's standard [Terms & Conditions](#) and the [Ethical guidelines](#) still apply. In no event shall the Royal Society of Chemistry be held responsible for any errors or omissions in this *Accepted Manuscript* or any consequences arising from the use of any information it contains.

Non-covalent functionalization of carbon nanotubes with boronic acids for the wiring of glycosylated redox enzymes in oxygen-reducing biocathodes

Bertrand Reuillard,^a Alan Le Goff,^a Michael Holzinger^a and Serge Cosnier^a

Cite this: DOI: 10.1039/x0xx00000x

Received 00th January 2012,
Accepted 00th January 2012

DOI: 10.1039/x0xx00000x

www.rsc.org/

We report the non-covalent functionalization of multiwalled carbon nanotubes with pyrene monomers bearing a boronic acid function. These functionalized electrodes were used to wire horseradish peroxidase via formation of a covalent boronic ester bond under mild conditions with the glycosylated enzyme. By attaching at the same time glucose oxidase, a bi-enzymatic system was elaborated and showed efficient bioelectrocatalytic oxygen reduction in physiological conditions.

Introduction

Bioelectrocatalytic reduction of substrates such as dioxygen or hydrogen peroxide by redox enzymes is one key step toward the development of efficient biocathodes in enzymatic biofuel cells (BFCs).^{1–4} In particular, glucose BFCs are envisioned for power harvesting from living organisms and thus, require low-overpotentials and high electrocatalytic oxygen reduction under physiological conditions, i.e. 5 mM glucose and 0.14 M NaCl.^{5–7} While multicopper enzymes are the most widely used enzymes for the reduction of O₂ at the biocathode, their sensitivity toward inhibitors such as chloride ions or urates complicates their use in implantable devices. Significant advances have recently been made by focusing on reducing H₂O₂ by horseradish peroxidase (HRP) immobilized on carbon nanotubes (CNTs) or on carbon microfibers.^{8,9} Thanks to an efficient direct electron transfer (DET) between HRP and the electrode, several examples demonstrate that HRP can electro-enzymatically reduce H₂O₂ into H₂O^{9,10} at low overpotentials (about +0.5 V vs SCE at pH 7). A bienzymatic system, combining HRP and glucose oxidase (GOx) has been envisioned to design novel oxygen-reducing biocathodes in the presence of glucose^{10,11}. GOx catalyzes the reduction of O₂ to H₂O₂ in presence of glucose while HRP reduces H₂O₂ into H₂O via DET. We recently demonstrated that this biocathode can

operate in a GBFC under physiological conditions¹⁰. Here, we took advantage of the glycosylated domain of both, GOx and HRP to bind these enzymes on boronic acid functionalized multiwalled carbon nanotubes (MWCNTs).

An elegant technique consists in the handy formation of boronic acid ester through the reaction of a boronic acid function on the electrode surface with the sugar residues of glycosylated proteins like GOx and HRP. Although this technique has widely been used for the immobilization of redox proteins on polymer backbones^{12,13} or via self-assembled monolayers^{14–17}, it was scarcely studied in combination with carbon nanotubes¹⁸. Most of the high-performance BFCs are using carbon nanotubes as conductive matrix. Indeed, their excellent electrochemical properties for electron transfers and their high specific surface are particularly attractive to immobilize and directly wire high amounts of enzymes.¹⁹ With the aim to develop a new MWCNT-based electrode with enhanced electrocatalytic properties towards the reduction of H₂O₂ and O₂ under mild conditions, this work describes the non-covalent functionalization of MWCNTs by pyrene derivatives bearing boronic acid. Two types of pyrene groups, with or without spacer, were used: pyrene-1-boronic acid (**pyrene 1**) and 1-(4-boronobenzyl)-3-(4-(pyren-1-yl)butanamido)pyridin-1-ium bromide (**pyrene 2**). The functionalization of MWCNT electrodes by HRP alone or by

GOX and HRP association was investigated for the catalytic reduction of H_2O_2 and O_2 , respectively.

Results and discussion

Direct electrochemistry of HRP immobilized on boronic acid-functionalized MWCNTs

MWCNT electrodes were obtained by the method from Wu et al.²⁰ that allows highly stable and reproducible MWCNT coating on GC electrodes. Using this transfer process, a homogenous and reproducible 4 μm -thick MWCNT film was obtained on the electrodes. The MWCNT electrodes are simply incubated for one hour in DMF containing **pyrene 1** or **pyrene 2** (10 mmol L^{-1}) and then incubated with the glycosylated enzymes in phosphate buffer solution (0.1 mol L^{-1} PBS, pH 7.4). In order to probe the DET between HRP and MWCNTs, we compared **pyrene 1** with no intermediary chain and **pyrene 2** with a semi-rigid spacer of about 10 \AA lengths. To address the efficiency of this covalent binding, we also performed the same experiments using 1-pyrenebutyric acid N-hydroxysuccinimide ester (**pyrene 3**). The latter forms a well-characterized amide coupling with amine residues at the surface of enzymes.

Scanning Electron Microscopy (SEM) images of the bioelectrodes confirm the high electroactive area of the electrodes and the excellent homogeneity of the MWCNT deposit (figure S1).

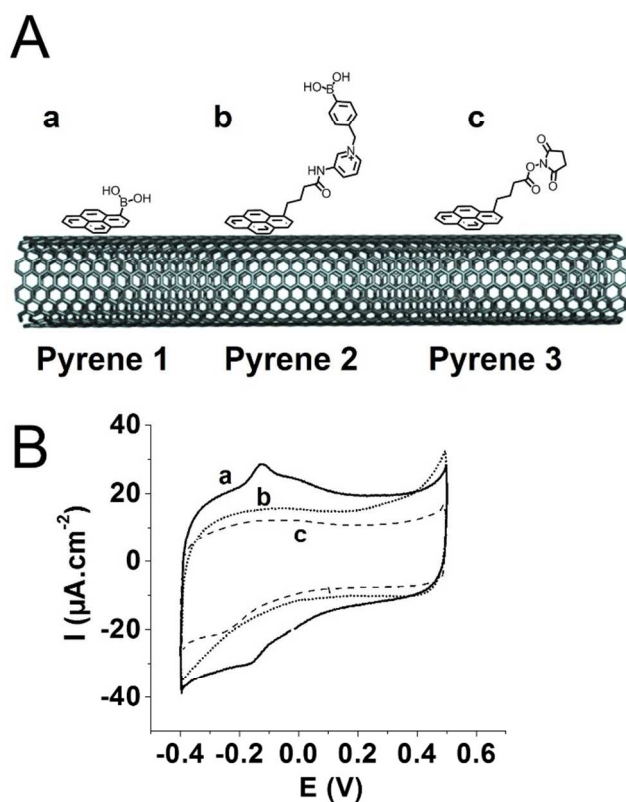


Figure 1. (A) Schematic representation of MWCNTs functionalized with (a) **pyrene 1**, (b) **pyrene 2** and (c) **pyrene 3**; (B) cyclic voltammograms of (a) **pyrene**

1, (b) **pyrene 2**- and (c) **pyrene 3**-functionalized bioelectrodes after incubation in a HRP containing PBS (0.1 mol L^{-1} pH 7.4) solution. The measurements were performed at a scan rate of 20 mV s^{-1} in 0.1 mol L^{-1} PBS, pH 7.4 at 25°C

The cyclic voltammograms of the bioelectrodes in PBS, exhibit a reversible redox system at $E_{1/2} = -0.10 \text{ V}$ ($\Delta E = 40 \text{ mV}$) vs SCE for the HRP electrode functionalized with **pyrene 1** (figure 1). This redox system is characteristic of the reversible $\text{Fe}^{3+}/\text{Fe}^{2+}$ redox process of the heme iron embedded in the protein and immobilized on the electrode. This reversible peak is not observed for the **pyrene 2** functionalized electrodes (Figure 1B). For **pyrene 3**, a poorly reversible system around -0.1V indicates the presence of directly-wired HRP. The MWCNT electrodes were then studied in presence and absence of 0.5 mmol L^{-1} H_2O_2 (Figure 2).

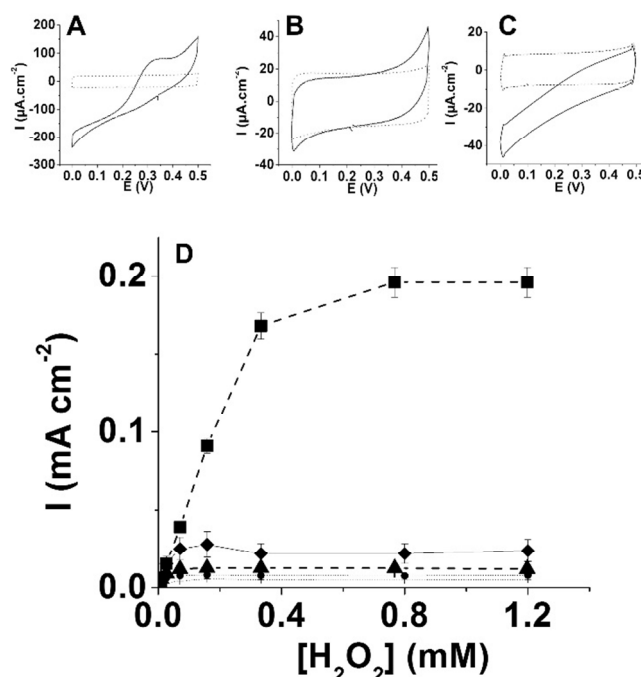


Figure 2. Cyclic voltammograms for MWCNT electrodes functionalized with HRP and (A) **pyrene 1**, (B) **pyrene 2** and (C) **pyrene 3** in the presence and absence of 1 mmol L^{-1} H_2O_2 ; (D) chronoamperometric experiments at $E_{\text{app}} = 0.2\text{V}$ for successive additions of H_2O_2 for MWCNT electrodes functionalized by (■) **pyrene 1**/HRP, (▲) **pyrene 2**/HRP, (◆) **pyrene 3**/HRP, (●) **pyrene butyric acid**/HRP and (+) only HRP (0.1 mol L^{-1} PBS, pH 7.4, 25°C , 20 mV s^{-1})

As expected from the previous experiment, a high catalytic current at low overpotential is especially observed for the **pyrene 1**-functionalized electrode. While **pyrene 2**-functionalized electrodes exhibits negligible H_2O_2 reduction, the **pyrene 3**-functionalized electrodes exhibits lower electrocatalytic properties towards H_2O_2 reduction compared to **pyrene 1**. The cyclic voltammogram exhibits an onset potential of $+0.43\text{V}$ for the electrocatalytic H_2O_2 reduction. This potential corresponds to the HRP Fe(IV)=O redox state of $+0.7\text{V}$ ²¹. This lower value arises from the competition between the electrocatalytic H_2O_2 reduction and H_2O_2 oxidation at the electrode^{9,10}. The electrocatalytic H_2O_2 oxidation process clearly appears in the anodic part of the CV from figure 2A at

around 0.2V. Chronoamperometric measurements have been carried out at $E = 0.2V$ with successive increments of H_2O_2 concentration (figure 2C). For **pyrene 1**, the electrocatalytic current reaches a maximum current density of $196 \mu A cm^{-2}$ at $0.8 mmol L^{-1}$ leading to a K_M^{app} value of $0.18 mmol L^{-1}$. This value is about half the value of the K_M of the enzyme free in solution, i.e. $0.44 mmol L^{-1}$ ²². This comparison reflects the efficiency of the electron transfer from MWCNT to the prosthetic site of the immobilized HRP compared to the enzyme in solution. In contrast, the **pyrene 2** functionalized electrodes involving a long spacer, show markedly lower maximum currents, namely $12 \mu A cm^{-2}$. **Pyrene 3**-functionalized electrodes exhibits maximum current of $28 \mu A cm^{-2}$, showing the lower electrocatalytic properties of these functionalized electrodes. We also performed control experiments by incubating HRP with both pristine MWCNT electrodes and MWCNT electrodes functionalized with 1-pyrene butyric acid in order to quantify unspecific binding of HRP. Both electrodes exhibits negligible catalytic currents for H_2O_2 reduction, namely 5 and $8 \mu A cm^{-2}$ respectively (figure 2D). Wiring of HRP via covalent binding to **pyrene 1** is particularly efficient compared to **pyrene 2** and **pyrene 3**. This efficiency likely arises from the high reactivity of boronic acids towards diol groups at the surface of the enzyme associated with the short length of the boronic acid linker.

These experiments demonstrates the formation of a hypervalent iron(IV)-oxo porphyrine oxidation state according to the presented mechanism shown in figure S2. To determine the amount of enzyme immobilized on the electrode and evaluate the influence of DET on the H_2O_2 reduction process, the enzymatic activity of the two different electrodes, was evaluated by a spectrophotometric assay. The HRP activity of an enzyme sample and bioelectrodes was measured by following the time-dependent appearance of the absorbance of the 2,2'-Azino-bis(3-ethylbenzothiazoline-6-sulfonic acid) diammonium radical cation ($ABTS^+$) at 415 nm under aerobic conditions. Assuming a straight that the enzyme has the same activity in its free or immobilized form, the comparison of the resulting activity indicates that 46 and $22 \mu g cm^{-2}$ of HRP were immobilized on **pyrene 1** and **pyrene 2**-functionalized MWCNTs, respectively (figure 3A, inset).

Compared to **pyrene 2**, it clearly appears that **pyrene 1** leads to the immobilization of a double amount of HRP with a markedly better electrical wiring. It should be noted that the theoretical maximum surface coverage with a close-packed HRP monolayer, calculated from its cross-sectional area, corresponds to $3.3 pmol cm^{-2}$ while voltammetric measurements provide a value of $3.8 pmol cm^{-2}$.²³ As a consequence, the HRP coverage ($46 \mu g cm^{-2}$) obtained with **pyrene 1**-functionalized MWCNTs is equivalent to the immobilization of 275-317 compact enzyme monolayers. This unambiguously illustrates the great advantage brought by the three-dimensional structure of the MWCNT matrix as well as the efficient anchoring of HRP within the whole structure. Taking into account that ABTS is also a well-known redox mediator for electrically connecting HRP to the electrode, we investigated, in parallel, the electrocatalytic

activity of the different electrodes in the presence of ABTS ($6 mmol L^{-1}$) by chronoamperometric measurements. The latter were performed at 0.2V and the measured maximum current densities are presented in figure 3A. The comparison of the catalytic current values (504 and $252 \mu A cm^{-2}$ for **pyrene 1** and **pyrene 2** MWCNT electrodes, respectively) corroborates the anchoring of a two time higher amount of enzyme via **pyrene 1**. In addition, for the **pyrene 1**-functionalized MWCNTs, a 2.5 fold increase of the catalytic current confirms that all of the immobilized HRP enzymes are not directly wired to the CNT matrix.

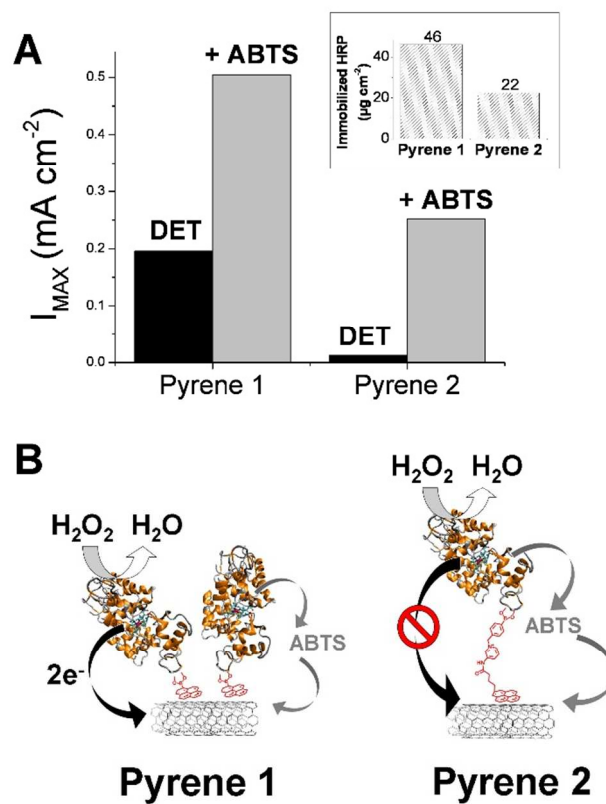


Figure 3. (A) Maximum current densities obtained by chronoamperometric experiments at $E_{app} = 0.2V$ in the presence of $1 mmol L^{-1} H_2O_2$ before and after addition of $6 mmol L^{-1} ABTS$ for **pyrene 1**/HRP and **pyrene 2**/HRP MWCNT electrodes ($0.1 mol L^{-1} PBS$ pH 7.4, $25^\circ C$); (inset) Amount of immobilized enzymes obtained by enzymatic activity measurements performed by UV-visible spectroscopy in the presence of ABTS; (B) Schematic representation of the electrocatalytic mechanism for **pyrene 1**/HRP and **pyrene 2**/HRP MWCNT electrodes

By assuming similar kinetics for DET and Mediated Electron Transfer (MET), we determined that about 40% of immobilized HRP are directly wired to the MWCNT electrode. For the **pyrene 2**-functionalized MWCNT electrodes, an electrocatalytic current of $252 \mu A cm^{-2}$ was measured in the presence of ABTS, indicating that only 5% HRP is directly wired. These experiments confirm firstly that boronic-acid groups are efficient anchors for covalent binding of glycosylated HRP on MWCNTs, and, secondly that the spacer length is of crucial importance. A short linkage is a prerequisite to provide an optimal distance between the heme domain of

HRP and the MWCNT sidewalls. Longer spacer groups prevent such close contacts to the electrode material that reduces drastically DET as depicted in figure 3B.

Co-immobilization of GOx and HRP for catalytic oxygen reduction

Taking advantage of the efficient DET observed between HRP and the MWCNT electrode functionalized with **pyrene 1**, a bienzymatic GOx-HRP system was elaborated for the enzymatic/electroenzymatic reduction of O_2 into H_2O via the H_2O_2 intermediate produced by GOx. **Pyrene 1**-functionalized MWCNTs were incubated in an aqueous solution containing equimolar amount of HRP and GOx (Figure 4).

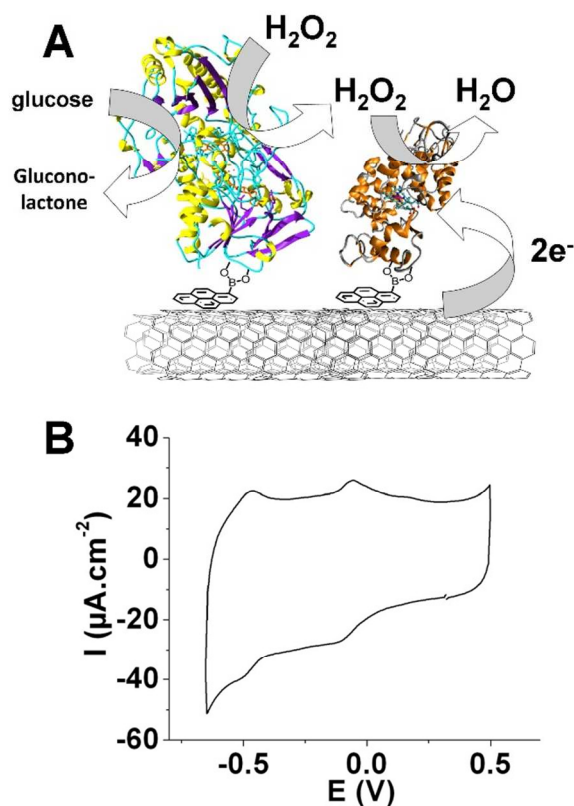


Figure 4. (A) Schematic representation of the functionalization of MWCNT electrodes with GOx and HRP for the reduction of O_2 into H_2O ; (B) cyclic voltammogram for MWCNT electrodes functionalized with **pyrene 1** after incubation in a $2\text{mg}\cdot\text{mL}^{-1}$ solution of equimolar GOx and HRP (0.1M PBS pH 7.4, 25°C , 20 mV s^{-1})

The cyclic voltammogram of the bienzymatic biocathode exhibits two reversible redox systems at -0.08V ($\Delta E = 50\text{mV}$) and -0.48 ($\Delta E = 46\text{mV}$), respectively (Figure 4B). These features correspond to the redox potentials of the HRP $\text{Fe}^{3+}/\text{Fe}^{2+}$ system and the FAD/FADH_2 cofactor of immobilized GOx. This redox behaviour demonstrates that both enzymes are linked to the MWCNTs surface *via* formation of boronic esters with **pyrene 1**.

In the presence of glucose (5 mmol L^{-1}), GOx oxidizes glucose to gluconolactone by reducing oxygen into H_2O_2 . The as produced H_2O_2 is then further reduced by HRP to water leading

to a catalytic reduction current with an onset potential of $+0.43\text{V}$ (figure 5A).

To optimize the bi-enzymatic biocathodes, the **pyrene 1** functionalized MWCNT electrodes were incubated in PBS containing different ratios of HRP/GOx (Figure 5B). Chronoamperometric measurements were carried out in PBS, pH7 at 37°C under successive additions of glucose at defined concentrations. Depending on the HRP/GOx ratio, different catalytic activities were observed. At low HRP/GOx ratio, the catalytic activity decreases for higher glucose concentrations. This effect is due to local overproduction of H_2O_2 by GOx that rapidly saturates and inhibits the enzymatic activity of HRP²³. At high HRP/GOx ratio, the higher number of wired HRP counterbalances this inhibition. Here, the catalytic activity steadily increases with the successive addition of glucose until a maximum current is obtained. This study underlines the excellent control over enzyme immobilization via the boronic ester linkage and, more importantly, the complicated mechanism for oxygen reduction induced by this bienzymatic system. Nevertheless, the optimal configuration of the bienzymatic system in physiological conditions, *i.e.* at 5 mmol L^{-1} glucose and 0.14 mol L^{-1} NaCl could be estimated. The optimal HRP/GOx ratio for these conditions is 10 that gave a catalytic current density of $10\mu\text{A cm}^{-2}$. A high ratio is needed to wire a maximum amount of HRP while a lower amount of GOx is necessary to limit the overproduction of H_2O_2 which inhibits HRP.

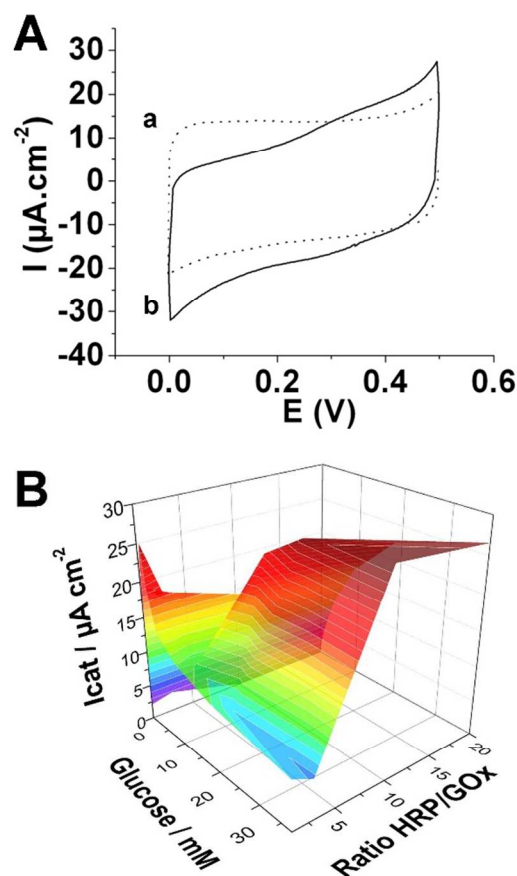


Figure 5. (A) Cyclic voltammograms for MWCNT electrodes functionalized with GOx and HRP in (a) absence and in (b) presence of 5mM glucose; (B) Evolution of the oxygen reduction catalytic current as a function of glucose concentration and HRP/GOx ratio ($E_{app} = 0.2V$, 0.1 mol L^{-1} PBS pH 7.4, 25°C , 20 mV s^{-1})

Conclusions

To conclude, this work shows the flexible and facile use of boronic acid-modified pyrene molecules to functionalize MWCNTs with glycosylated enzymes. Excellent HRP wiring could be achieved accompanied with efficient electrocatalytic reduction of H_2O_2 . In combination with co-immobilized GOx under the same boronic ester linker, a biocathode for low-overpotential reduction of O_2 was designed which is operational under physiological conditions, i.e. at 5 mmol L^{-1} glucose and 0.14 mmol L^{-1} NaCl. Such bioelectrodes have therefore clear advantages compared to biocathodes using multicopper enzymes for the electrocatalytic reduction of oxygen. This setup could be more appropriate in glucose/ O_2 biofuel cells, designated for implantation in order to supply electronic medical devices with energy out of body liquids.

Experimental

General procedures

Glucose oxidase (from *Aspergillus niger*, $139 \text{ units mg}^{-1}$), Horseradish peroxidase ($730 \text{ units mg}^{-1}$), 1-pyrene boronic acid, N-hydroxyl succinimid (NHS), 1-Hydroxybenzotriazole hydrate (HOBt), 4-(Bromomethyl)phenylboronic acid, 1-pyrenebutyric acid, 1-pyrenebutyric acid N-hydroxysuccinimide ester and dimethylformamide (DMF) were purchased from Sigma Aldrich. 1-pyrene butyric acid and 3-aminopyridine were purchased from Alfa Aesar. The synthesis of **pyrene 2** was done as previously described²⁴. When not used, the enzymes were stored at 4°C . All reagents were used as received without any further purification. Electrochemical measurements were carried out using a Biologic VMP3 Multi Potentiostat. A Pt grid was used as counter electrode and a saturated calomel electrode was used as reference electrode. PBS pH 7.4 was used as electrolyte.

UV/Vis experiments were run on a Perkin Elmer UV/Vis spectrometer Lambda 650.

Preparation of bioelectrodes

For the preparation of the bioelectrodes, commercial grade Multi-Walled Carbon Nanotubes (9.5 nm diameter, purity > 95%) were obtained from Nanocyl. MWCNTs films were prepared using a modified procedure from Wu et al.²⁰. MWCNTs (10 mg) were dispersed in 500 mL of pure water and sonicated for 30 min. After the solution was let to decant overnight, the remaining transparent supernatant (400 mL) was filtered over cellulose nitrate filter (Sartorius, $0.45 \mu\text{m}$, $\varnothing 3.5 \text{ cm}$). The resulting deposit of MWCNTs was then deposited on a GC electrode (surface area 0.07 cm^2) and the filter membrane was then carefully dissolved with acetone.

Non-covalent immobilization of the pyrene residues was carried out by incubation of the MWCNTs electrodes in a 10 mmol L^{-1} solution of **pyrene 1** or **pyrene 2** in DMF. Pi-stacking process was let to react for 1h and the electrodes were then rinsed several times in DMF and then in pure water. The functionalized electrodes were then incubated overnight in a 2 mg mL^{-1} PBS containing HRP or a HRP/GOx mixture (according to the functionalization process) at pH 8 at 4°C . Then, the electrodes were rinsed and kept in PBS when not used. The MWCNT bioelectrodes were used as working electrodes (3mm diameter).

Acknowledgements

The Région Rhones-Alpes is acknowledged for the PhD funding of B. Reuillard. The present work was also partially supported by the Labex ARCANE (ANR-11-LABX-0003-01). The authors are also grateful to the scientific structure 'Nanobio' for providing facilities. The authors also thank the the ANR Investissements d'avenir – Nanobiotechnologies 10-IANN-0-02 programs for financial support.

Notes and references

^a Département de Chimie Moléculaire (DCM), UMR-5250, CNRS-UJF 570 rue de la Chimie, BP 53, 38041 Grenoble, France E-mail: serge.cosnier@ujf-grenoble.fr.

Electronic Supplementary Information (ESI) available: [Figure S1 and S2]. See DOI: 10.1039/c000000x/

1. S. C. Barton, J. Gallaway, and P. Atanassov, *Chem. Rev.*, 2004, **104**, 4867–4886.
2. W. Gellert, M. Kesmez, J. Schumacher, N. Akers, and S. D. Minteer, *Electroanalysis*, 2010, **22**, 727–731.
3. J. A. Cracknell, K. A. Vincent, and F. A. Armstrong, *Chem Rev*, 2008, **108**, 2439–2461.
4. I. Willner, Y. -M Yan, B. Willner, and R. Tel-Vered, *Fuel Cells*, 2009, **9**, 7–24.
5. E. Katz and K. MacVittie, *Energy Environ. Sci.*, 2013, **6**, 2791–2803.
6. A. Zebda, S. Cosnier, J.-P. Alcaraz, M. Holzinger, A. Le Goff, C. Gondran, F. Boucher, F. Giroud, K. Gorgy, H. Lamraoui, and P. Cinquin, *Sci. Rep.*, 2013, **3**.
7. S. Cosnier, A. Le Goff, and M. Holzinger, *Electrochem. Commun.*, 2014, **38**, 19–23.
8. Y.-D. Zhao, W.-D. Zhang, H. Chen, Q.-M. Luo, and S. F. Y. Li, *Sens. Actuators B Chem.*, 2002, **87**, 168–172.
9. W. Jia, S. Schwamborn, C. Jin, W. Xia, M. Muhler, W. Schuhmann, and L. Stoica, *Phys. Chem. Chem. Phys.*, 2010, **12**, 10088–10092.
10. C. Agnès, B. Reuillard, A. Le Goff, M. Holzinger, and S. Cosnier, *Electrochem. Commun.*, 2013, **34**, 105–108.
11. W. Jia, C. Jin, W. Xia, M. Muhler, W. Schuhmann, and L. Stoica, *Chem. – Eur. J.*, 2012, **18**, 2783–2786.
12. Y. Huang, W. Wang, Z. Li, X. Qin, L. Bu, Z. Tang, Y. Fu, M. Ma, Q. Xie, S. Yao, and J. Hu, *Biosens. Bioelectron.*, 2013, **44**, 41–47.
13. S. Liu, L. Bakovic, and A. Chen, *J. Electroanal. Chem.*, 2006, **591**, 210–216.

14. J. M. Abad, M. Vélez, C. Santamaría, J. M. Guisán, P. R. Matheus, L. Vázquez, I. Gazaryan, L. Gorton, T. Gibson, and V. M. Fernández, *J. Am. Chem. Soc.*, 2002, **124**, 12845–12853.
 15. S. Liu, U. Wollenberger, J. Halánek, E. Leupold, W. Stöcklein, A. Warsinke, and F. W. Scheller, *Chem. – Eur. J.*, 2005, **11**, 4239–4246.
 16. M. Zayats, E. Katz, and I. Willner, *J. Am. Chem. Soc.*, 2002, **124**, 14724–14735.
 17. M. Zayats, E. Katz, and I. Willner, *J. Am. Chem. Soc.*, 2002, **124**, 2120–2121.
 18. B. Mu, T. P. McNicholas, J. Zhang, A. J. Hilmer, Z. Jin, N. F. Reuel, J.-H. Kim, K. Yum, and M. S. Strano, *J. Am. Chem. Soc.*, 2012, **134**, 17620–17627.
 19. M. Holzinger, A. Le Goff, and S. Cosnier, *Electrochimica Acta*, 2012, **82**, 179–190.
 20. Z. Wu, Z. Chen, X. Du, J. M. Logan, J. Sippel, M. Nikolou, K. Kamaras, J. R. Reynolds, D. B. Tanner, A. F. Hebard, and A. G. Rinzler, *Science*, 2004, **305**, 1273–1276.
 21. G. I. Berglund, G. H. Carlsson, A. T. Smith, H. Szöke, A. Henriksen, and J. Hajdu, *Nature*, 2002, **417**, 463–468.
 22. A. D. Ryabov, V. N. Goral, L. Gorton, and E. Csöregi, *Chem. – Eur. J.*, 1999, **5**, 961–967.
 23. B. Limoges, J.-M. Savéant, and D. Yazidi, *J. Am. Chem. Soc.*, 2003, **125**, 9192–9203.
 24. Y.-J. Huang, W.-J. Ouyang, X. Wu, Z. Li, J. S. Fossey, T. D. James, and Y.-B. Jiang, *J. Am. Chem. Soc.*, 2013, **135**, 1700–1703.
-